General Disclaimer

One or more of the Following Statements may affect this Document

- This document has been reproduced from the best copy furnished by the organizational source. It is being released in the interest of making available as much information as possible.

- This document may contain data, which exceeds the sheet parameters. It was furnished in this condition by the organizational source and is the best copy available.

- This document may contain tone-on-tone or color graphs, charts and/or pictures, which have been reproduced in black and white.

- This document is paginated as submitted by the original source.

- Portions of this document are not fully legible due to the historical nature of some of the material. However, it is the best reproduction available from the original submission.

NASA Technical Memorandum 78469

Conservative Implicit Schemes for the Full Potential Equation Applied to Transonic Flows

Terry L. Holst and William F. Ballhaus

March 1978

NASA

NASA Technical Memorandum 78469

CONSERVATIVE IMPLICIT SCHEMES FOR THE FULL POTENTIAL EQUATION APPLIED TO TRANSONIC FLOWS

Terry L. Holst
Ames Research Center
Moffett Field, Calif. 94035

and

William F. Ballhaus
Aeromechanics Laboratory
U.S. Army Aviation R&D Command
Ames Research Center
Moffett Field, Calif. 94035

CONSERVATIVE IMPLICIT SCHEMES FOR THE FULL POTENTIAL EQUATION APPLIED TO TRANSONIC FLOWS

Terry L. Holst
Ames Research Center

and

William F. Ballhaus
Aeromechanics Laboratory
U.S. Army Aviation R&D Command

SUMMARY

Implicit approximate factorization techniques (AF) are investigated for the solution of matrix equations resulting from finite-difference approximations to the full potential equation in conservation form. For transonic flows, an artificial viscosity, required to maintain stability in supersonic regions, is introduced by an upwind bias of the density. Two implicit AF procedures are presented and their convergence performance is compared with that of the standard transonic solution procedure, successive line overrelaxation (SLOR). Subcritical and supercritical test cases are considered. The results indicate that the AF schemes are substantially faster than SLOR.

I. INTRODUCTION

There are basically three formulations for inviscid transonic flows. These are, in order of increasing complexity (and in order of decreasing approximation): (1) transonic small disturbance potential equation (TSD), (2) full potential equation (FP), and (3) Euler equations (exact inviscid formulation). TSD is valid for thin wings at free-stream Mach numbers near unity and is an isentropic and irrotational formulation. It offers the advantage of simplicity, especially in the treatment of wing surface boundary conditions. The FP formulation can be considered exact under the assumptions of irrotational and isentropic flow. These assumptions, which are less restrictive than those for TSD, are valid for a wide range of practical transonic flows. Potential formulations can be written in terms of a single second-order partial differential equation (PDE), whereas the Euler formulation consists of a set of first order PDE's (usually four in two-dimensional cases). Hence, for implicit AF schemes the potential formulations require only scalar matrix operations, while the Euler formulation requires time-consuming block matrix operations. The FP formulation is the most efficient of the three formulations in terms of accuracy-to-cost ratio for the majority of inviscid transonic flow applications.

The object of this investigation has been to determine the feasibility of using implicit approximate factorization algorithms (AF) to solve the full

potential equation in conservation form for steady transonic flow fields. The two AF schemes tested are logical extensions of the schemes previously developed for the TSD equation (refs. 1,2). These previous studies found the AF approach to be substantially faster than the standard transonic flow field solution procedure, successive line overrelaxation (SLOR).

Section II begins with a discussion of the full potential equation in conservation form. Spatial difference approximations are then introduced, including the addition of artificial viscosity required to maintain stability in supersonic zones. The difference approximations are equivalent to those introduced by Jameson (ref. 3). Here, however, the artificial viscosity is not introduced explicitly, as in the Jameson approach, but rather by retarding the density.

In Section III, two implicit AF iteration schemes are presented. AF and SLOR convergence histories are then compared in Section IV for both subcritical and supercritical cases. Results indicate a substantial increase in computational efficiency for the AF schemes over an SLOR scheme.

The authors express their gratitude to Joseph L. Steger for his many helpful suggestions during the course of this study.

II. SPATIAL DIFFERENCING OF THE FULL POTENTIAL EQUATION IN CONSERVATION FORM

A. The Full Potential Equation

The full potential equation written in conservation-law form is given by

$$(\rho\phi_x)_x + (\rho\phi_y)_y = 0 \tag{1}$$

where

$$\rho = \left[1 - \frac{\gamma - 1}{\gamma + 1}\left(\phi_x^2 + \phi_y^2\right)\right]^{1/\gamma-1} \tag{2}$$

In equations (1) and (2) the density (ρ) and velocity components (ϕ_x and ϕ_y) are nondimensionalized by the stagnation density (ρ_s) and the critical sound speed (a_*), respectively, x and y are Cartesian coordinates, and γ is the ratio of specific heats. In addition, other useful relations nondimensionalized by ρ_s and a_* are given by

$$\frac{q^2}{2} + \frac{a^2}{\gamma - 1} = \frac{1}{2}\frac{\gamma + 1}{\gamma - 1} \tag{3}$$

$$p = \frac{\gamma + 1}{2\gamma}\rho^\gamma \tag{4}$$

$$a^2 = \frac{\gamma p}{\rho} \tag{5}$$

where q is the flow speed $\left(\sqrt{\phi_x^2 + \phi_y^2}\right)$, a is the speed of sound and p is the pressure.

Equations (1) and (2) express mass conservation for flows that are isentropic and irrotational. The corresponding shock-jump conditions are valid approximations to the Rankine-Hugoniot relations for many transonic flow applications. A comparison of the isentropic and Rankine-Hugoniot shock polars is given in reference 4.

It is essential that the finite difference approximation to equation (1) be cast in conservation form (ref. 5). Otherwise, the shock capturing procedure will not necessarily conserve mass across the shock wave (ref. 3). Nonconservative rather than conservative difference schemes have been used in many engineering applications. However, the nonconservative procedures introduce mass sources at shock waves, and the strength of these sources depends on the local grid spacing, a nonphysical consideration. Erroneous shock solutions therefore result.

B. Spatial Differencing in One Dimension

To begin with, consider the one-dimensional version of equation (1),

$$(\rho\phi_x)_x = 0 \tag{6}$$

A second-order accurate finite-difference approximation to equation (6) is given by

$$\overleftarrow{\delta}_x \rho_{i+(1/2)} \overrightarrow{\delta}_x \phi_i = 0 \tag{7}$$

where $\overleftarrow{\delta}_x$ and $\overrightarrow{\delta}_x$ are backward and forward difference operators defined by

$$\begin{aligned} \overleftarrow{\delta}_x \phi_i &= \Delta x^{-1}(\phi_i - \phi_{i-1}) \\ \overrightarrow{\delta}_x \phi_i &= \Delta x^{-1}(\phi_{i+1} - \phi_i) \end{aligned} \tag{8}$$

Equation (7) is a suitable finite-difference scheme for subsonic flow regions; however, for supersonic regions, a properly-chosen artificial viscosity term must be added. For example, Jameson (ref. 3) adds the following viscosity term:

$$-(\mu\phi_{xx})_x \tag{9}$$

where $\mu = \min[0, \rho(1 - \phi_x^2/a^2)]$. This is analogous to the switching used in the Murman mixed-difference procedure (ref. 6). It can be shown (ref. 3) (by differentiating the one-dimensional form of equation (2)) that this is equivalent to adding

$$-(\nu\rho_x\phi_x)_x \tag{10}$$

where $\nu = \max[0,(1 - a^2/\phi_x{}^2)]$. The complete finite-difference approximation to equation (6) can thus be written

$$(\rho\phi_x)_x \approx \overleftarrow{\delta}_x \rho_{i+(1/2)} \overrightarrow{\delta}_x \phi_i - \overleftarrow{\delta}_x \nu_i [\rho_{i+(1/2)} - \rho_{i-(1/2)}] \overrightarrow{\delta}_x \phi_i = 0 \qquad (11)$$

(Other difference approximations to equation (10) are possible, and some of these will be discussed in a subsequent section.) This scheme is centrally differenced and second-order accurate in subsonic regions. In supersonic regions, the differencing is a combination of the second-order accurate central differencing used in subsonic regions and the first-order accurate upwind differencing resulting from the addition of artificial viscosity. As the flow becomes increasingly supersonic, the scheme is increasingly retarded in the upwind direction.

Equation (11) can be rearranged to give

$$(\rho\phi_x)_x \approx \overleftarrow{\delta}_x \tilde{\rho}_{i+(1/2)} \overrightarrow{\delta}_x \phi_i = 0 \qquad (12a)$$

where

$$\tilde{\rho}_{i+(1/2)} = (1 - \nu_i)\rho_{i+(1/2)} + \nu_i \rho_{i-(1/2)} \qquad (12b)$$

The addition of the artificial viscosity given by equation (10) is thus equivalent to retarding the density in equation (7). Artificial viscosity is not added explicitly as in the Jameson (ref. 3) procedure. However, the two approaches produce identical results. The significance of the present approach will become apparent in the discussion of solution algorithms (Section III).

The choice of ν strongly affects the accuracy and stability of solutions to equation (12). The particular choice $\nu = \max[(1 - a^2/\phi_x{}^2),0]$ results in an effective artificial viscosity that corresponds exactly to the form used by Jameson (ref. 3), and generally satisfactory results are obtained. For $\nu = 0$, the difference scheme reduces to equation (7), which is unstable for supersonic regions. The choice $\nu = 1$ results in a first-order-accurate approximation that is highly dissipative. However, stable solutions can be obtained for both subsonic and supersonic regions. Thus, by sacrificing second-order accuracy in subsonic regions, a scheme can be constructed that need <u>not</u> be switched in the Murman fashion. Moreover, accuracy can be improved somewhat by decreasing ν. However, in supersonic regions a stability limit is encountered for values well above zero. Computed results for various choices of ν are presented in the following section.

C. Computed Results for the One-Dimensional Case

The effect of ν on shock wave resolution is studied here using a one-dimensional test problem illustrated in figure 1. A uniform grid spacing of unity is used. Boundary conditions are

$$\left.\begin{aligned} \phi(0) &= 0 \\ \phi_x(0) &= U_\infty \\ \phi(XMAX) &= \phi_{NI} \text{ (specified)} \end{aligned}\right\} \tag{13}$$

The slope discontinuity in the ϕ distribution represents a shock wave. The flow upstream and downstream of the shock is uniform.

Computed results are shown in figure 2. Three different shock strengths are presented, corresponding to three different choices of U_∞. Exact (discontinuous) solutions are indicated by the dashed line. The discrete data are solutions to equation (12) for three different choices of ν, representing three different strategies for choosing a value of artificial viscosity by retarding the density. The result equivalent to the Jameson viscosity, which is switched on (in the Murman fashion) only for supersonic points, is shown by the triangles. There is a slight overshoot that increases in amplitude with increasing shock strength. Note that the shock is always captured in a distance of about three mesh cell widths.

The two other solutions were computed with ν constant. The density is retarded by the same amount in both subsonic and supersonic regions, so that there is no Murman-type switching. The solutions represented by the squares were computed using a constant value of ν equivalent to that used in the (uniform) supersonic region by the Jameson strategy. Shock waves for this approach are captured in about five to seven mesh cell widths. For the choice $\nu = 1$, shocks are smeared over a substantially greater distance, especially for the weaker shocks.

The results shown in figure 2 indicate that the Jameson choice of artificial viscosity, implemented here by retarding the density, is a suitable one for shocks of weak to moderate strength. Furthermore, if one is willing to sacrifice second-order accuracy in subsonic regions and accept a greater degree of shock smearing, solutions can be obtained without switching differences; the test for supersonic flow can thereby be eliminated.

D. Spatial Differences in Two Dimensions

A second-order accurate finite-difference approximation to equation (1) is given by

$$[\overleftarrow{\delta}_x \rho_{i+(1/2),j} \vec{\delta}_x + \overleftarrow{\delta}_y \rho_{i,j+(1/2)} \vec{\delta}_y] \phi_{i,j} = 0 \tag{14}$$

where $\overleftarrow{\delta}_y$ and $\vec{\delta}_y$ are backward and forward y-direction difference operators, respectively, defined similarly to the x-direction operators given by equation (8). As in the one-dimensional case, equation (14) is a suitable finite-difference scheme for subsonic flow regions but not for supersonic flow regions. A properly chosen artificial viscosity term must be added. In two dimensions, Jameson (ref. 3) adds an artificial viscosity term of the following form ($u_{i+(1/2),j} > 0$, $v_{i,j+(1/2)} > 0$)

$$-\overleftarrow{\delta}_x \nu_{i,j} u_{i+(1/2),j} \rho_{x_{i,j}} - \overleftarrow{\delta}_y \nu_{i,j} v_{i,j+(1/2)} \rho_{y_{i,j}} \tag{15a}$$

where $\nu = \max[0,(1 - a^2/q^2)]$. For the case when $v_{i,j+(1/2)} < 0$ the artificial viscosity term is slightly different and is given by

$$-\overleftarrow{\delta}_x \nu_{i,j} u_{i+(1/2),j} \rho_{x_{i,j}} - \overleftarrow{\delta}_y \nu_{i,j+1} v_{i,j+(1/2)} \rho_{y_{i,j+1}} \tag{15b}$$

Other cases arise when $u_{i+(1/2),j} < 0$ and are handled in a similar fashion. For convenience of presentation, only the first case will be considered hereafter. The complete finite-difference approximation to equation (1) can thus be written

$$(\rho\phi_x)_x + (\rho\phi_y)_y \approx [\overleftarrow{\delta}_x \rho_{i+(1/2),j} \overrightarrow{\delta}_x + \overleftarrow{\delta}_y \rho_{i,j+(1/2)} \overrightarrow{\delta}_y]\phi_{i,j}$$
$$- \overleftarrow{\delta}_x \nu_{i,j} u_{i+(1/2),j} \rho_{x_{i,j}} - \overleftarrow{\delta}_y \nu_{i,j} v_{i,j+(1/2)} \rho_{y_{i,j}} = 0 \tag{16}$$

This scheme is centrally differenced and second-order accurate in subsonic regions. In supersonic regions, the differencing is a combination of the second-order accurate central differencing used in subsonic regions and the first-order accurate upwind differencing resulting from the addition of artificial viscosity. As the flow becomes increasingly supersonic, the scheme is increasingly retarded in the upwind direction.

As in the one-dimensional case, the two-dimensional scheme can be rearranged to give

$$(\rho\phi_x)_x + (\rho\phi_y)_y \approx [\overleftarrow{\delta}_x \tilde{\rho}_{i+(1/2)} \overrightarrow{\delta}_x + \overleftarrow{\delta}_y \bar{\rho}_{j+(1/2)} \overrightarrow{\delta}_y]\phi_{i,j} = 0 \tag{17a}$$

$$\tilde{\rho}_{i+(1/2)} = (1 - \nu_{i,j})\rho_{i+(1/2),j} + \nu_{i,j}\rho_{i-(1/2),j} \tag{17b}$$

$$\bar{\rho}_{j+(1/2)} = (1 - \nu_{i,j})\rho_{i,j+(1/2)} + \nu_{i,j}\rho_{i,j-(1/2)} \tag{17c}$$

The addition of the artificial viscosity given by equation (15) is thus equivalent to retarding the density in equation (14). Artificial viscosity is not added explicitly as in the Jameson procedure. However, the two approaches produce identical results. As pointed out by Jameson (ref. 3), the difference scheme given by equation (16) provides automatic upwind differencing of the streamwise terms in supersonic regions. Thus the full effect of rotated differencing is included in the present finite-difference scheme.

The present scheme can easily be extended to include an arbitrary coordinate system. For example, transformation of the full potential equation from Cartesian coordinates (x,y) given by equation (1) to a general coordinate system (ξ,η) yields the full potential equation in the following form:

$$\left(\frac{\rho U}{J}\right)_\xi + \left(\frac{\rho V}{J}\right)_\eta = 0 \tag{18}$$

where J is the Jacobian of the transformation and U and V are the contravariant velocities along the ξ and η directions, respectively, which are defined by

$$\left.\begin{aligned} U &= A_1\phi_\xi + A_2\phi_\eta \\ V &= A_2\phi_\xi + A_3\phi_\eta \end{aligned}\right\} \tag{19}$$

A_1, A_2, and A_3 are metric coefficients which depend on the type of transformation. No restrictions have been placed on the (ξ,η) coordinate system, and, for example, nonorthogonal coordinates can be used. This allows considerable flexibility in treating a wide range of geometries.

The spatial differencing scheme for a general (ξ,η) coordinate system can be written as follows

$$\left(\frac{\rho U}{J}\right)_\xi + \left(\frac{\rho V}{J}\right)_\eta \approx \delta_\xi^{\mp}\tilde{\rho}_{i+(1/2)}\left(\frac{U}{J}\right)_{i+(1/2),j} + \delta_\eta^{\mp}\bar{\rho}_{j+(1/2)}\left(\frac{V}{J}\right)_{i,j+(1/2)} = 0 \tag{20}$$

where $\tilde{\rho}_{i+(1/2)}$ and $\bar{\rho}_{j+(1/2)}$ are defined as before by equation (17). The general spatial difference scheme given by equation (20) contains all of the properties of the simpler Cartesian version (eq. (17)). Namely, this scheme is second-order accurate and centrally differenced in subsonic flow regions. The artificial viscosity is obtained solely by an upwind bias of the density coefficient in both the ξ and η directions. This form of spatial differencing fits nicely into the framework of many iteration procedures. Three procedures will be presented and tested in subsequent sections of this report. For the sake of simplicity, only the Cartesian form of the full potential equation will be investigated.

III. IMPLICIT APPROXIMATE FACTORIZATIONS

A. General Requirements

The finite-difference approximation to the full potential equation introduced in the previous section (eq. (17a)) can be written

$$L\phi = 0 \tag{21}$$

and is applied to every mesh cell in the flow field. The purpose of this section is to describe several iteration procedures for solving the resulting matrix equation to determine ϕ (and thus ρ) at each mesh point.

A general form for a two-level solution procedure is given by

$$NC^n + \omega R^n = 0 \tag{22}$$

where $C^n(=\phi^{n+1} - \phi^n)$ is the correction, $R^n(=L\phi^n)$ is the residual, which is a measure of how well the finite-difference equation is satisfied by the nth level solution (ϕ^n), and ω is a relaxation parameter. The iteration scheme given by equation (22) can be regarded as an iteration in pseudo-time, where the n superscript indicates the time-step level of the solution.

The operator N determines the type of iterative procedure and, therefore, determines the rate at which the solution procedure converges. In the approximate factorization approach N is chosen as a product of two or more factors indicated by

$$N = N_1 \cdot N_2 \sim L \tag{23}$$

The factors N_1 and N_2 are chosen so that: (1) their product is an approximation to L, (2) only simple matrix operations are required, and (3) the overall scheme is stable.

In what follows, three iteration procedures are discussed, each corresponding to a different choice for N. These methods, which involve only simple bidiagonal or tridiagonal matrix operations, are: (1) successive line overrelaxation (SLOR), the standard transonic flow solution procedure; (2) alternating direction implicit (ADI), one type of implicit approximate factorization scheme (called AF1 in ref. 1); and (3) AF2, another type of implicit approximate factorization scheme.

B. Successive Line Overrelaxation (SLOR)

The SLOR algorithm used in the present study can be expressed by choosing N as follows

$$NC^n_{i,j} = \left[\Delta x^{-1}\left(-\frac{\tilde{\rho}^n_{i+(1/2)}}{\Delta x} - \tilde{\rho}^n_{i-(1/2)}\overleftarrow{\delta}_x\right) + \overleftarrow{\delta}_y\bar{\rho}^n_{j+(1/2)}\overrightarrow{\delta}_y\right]C^n_{i,j} \tag{24}$$

This difference expression has been time-linearized by evaluating ρ at iteration level n. Because the cross terms are indirectly included in ρ, the form of N chosen here is simpler than the commonly used quasi-linear form of the full potential equation. This scheme is implicit in the y direction; that is, the complete y-direction operator is included in N. This requires the inversion of a tridiagonal matrix equation for each x = constant line. The operator is explicit in the x direction because it contains only the lower diagonal part of the x-direction operator. This means that each grid point is influenced by only a single grid point to the right in the x direction during one iteration, which contributes to a relatively slow evolution of the solution. Construction of N in a fully implicit manner, however, means that each grid point is influenced by every other grid point during each iteration. As a result, much faster convergence can be obtained. The next two algorithms presented are both fully implicit and obtain this form by constructing N as approximate factorizations of L.

C. Approximate Factorization, Scheme 1 (AF1)

The first fully implicit algorithm is similar to the AF1 scheme presented in reference 1, which was used to solve the TSD equation. This scheme, which is a reformulation of the Peaceman-Rachford alternating direction implicit technique (ADI), can be expressed by choosing N as follows:

$$\alpha NC^n_{i,j} = -\left(\alpha - \overleftarrow{\delta}_x \tilde{\rho}^n_{i+(1/2)} \overrightarrow{\delta}_x\right)\left(\alpha - \overleftarrow{\delta}_y \bar{\rho}^n_{j+(1/2)} \overrightarrow{\delta}_y\right) C^n_{i,j} \tag{25}$$

where α is a free parameter to be defined subsequently. Note that both the x and y directions are treated implicitly and that N has been written as the product of two factors which when multiplied out yield

$$\alpha NC^n_{i,j} = -\alpha^2 C^n_{i,j} - \overleftarrow{\delta}_x \tilde{\rho}^n_{i+(1/2)} \overrightarrow{\delta}_x \overleftarrow{\delta}_y \bar{\rho}^n_{j+(1/2)} \overrightarrow{\delta}_y C^n_{i,j} + \alpha LC^n_{i,j} \tag{26}$$

This expression includes the time-linearized L operator plus two error terms. The first error term is a ϕ_t-type term and therefore, provides a stabilizing effect to the iteration process in subsonic flow regions but a destabilizing effect in supersonic flow regions (ref. 7). The effect of this term is apparent in the computed results, Section IV.

The scheme can be restated in practical terms using two steps as follows

<u>step 1</u>:
$$\left[\alpha - \overleftarrow{\delta}_x \tilde{\rho}^n_{i+(1/2)} \overrightarrow{\delta}_x\right] f^n_{i,j} = \alpha\omega L\phi^n_{i,j} \tag{27a}$$

<u>step 2</u>:
$$\left[\alpha - \overleftarrow{\delta}_y \bar{\rho}^n_{j+(1/2)} \overrightarrow{\delta}_y\right] C^n_{i,j} = f^n_{i,j} \tag{27b}$$

where ω is a relaxation parameter and $f^n_{i,j}$ is an intermediate result stored at each mesh point in the finite difference mesh. In step 1 the f array is obtained by solving a tridiagonal matrix equation for each y = constant line. The correction array ($C^n_{i,j}$) is then obtained in the second step from the f array by solving a tridiagonal matrix equation for each x = constant line. Thus by writing N as the product of two factors it is possible to obtain a fully implicit technique involving only simple tridiagonal matrix operations.

D. Approximate Factorization, Scheme 2 (AF2)

The second fully implicit algorithm presented here is similar to the AF2 scheme presented in reference 1, which was applied to the TSD equation. The AF2 scheme, first investigated by Ballhaus and Steger (ref. 8) for unsteady flows, can be expressed by choosing N as follows:

$$\alpha NC^n_{i,j} = -\left(\alpha\overleftarrow{\delta}_x - \overleftarrow{\delta}_y \bar{\rho}^n_{j+(1/2)} \overrightarrow{\delta}_y\right)\left(\alpha - \tilde{\rho}^n_{i+(1/2)} \overrightarrow{\delta}_x\right) C^n_{i,j} \tag{28}$$

where again N has been written as the product of two factors, which, when multiplied out, yield the time-linearized L operator plus two error terms. The first error term is an upwind ϕ_{xt}-type term and therefore, provides time-dependent dissipation for the convergence process, which is especially convenient for supersonic flow. When constructing N in this form, care must be taken to ensure that this term has the proper sign and is differenced in the upwind direction. Implementation of the AF2 scheme is achieved by writing it in a two step form given by

$$\underline{\text{step 1}}: \qquad \left(\alpha\vec{\delta}_x - \overleftarrow{\delta}_y \bar{\rho}^n_{j+(1/2)} \vec{\delta}_y\right) f^n_{i,j} = \alpha\omega L\phi^n_{i,j} \tag{29a}$$

$$\underline{\text{step 2}}: \qquad \left(\alpha - \tilde{\rho}^n_{i+(1/2)} \overleftarrow{\delta}_x\right) C^n_{i,j} = f^n_{i,j} \tag{29b}$$

where ω is a relaxation parameter and $f^n_{i,j}$ is an intermediate result stored at each mesh point in the finite difference mesh. In step 1, the f array is obtained by solving a tridiagonal matrix equation for each x = constant line. The correction array ($C^n_{i,j}$) is then obtained in the second step from the f array by solving a simple bidiagonal matrix equation for each y = constant line. Note that with AF2 the x-direction difference approximation is split between the two steps. This generates the desired ϕ_{xt} term as mentioned above and also places a sweep direction restriction on both steps, namely, downwind for the first step and upwind for the second step.

Several variations of the AF2 scheme are possible. Some of these include: (1) splitting the y-direction term instead of the x-direction term, (2) changing the order of the steps, and (3) moving the x-direction density coefficient ($\tilde{\rho}^n_{i+(1/2)}$) from the second factor to the first factor. These three variations have been tried and were found to be stable.

Normally, flow-field, type-dependent differencing is used to achieve stability in transonic flow calculations. Incorporating these different operators into iteration procedures, such as the AF schemes presented here, would be cumbersome if not impossible. Using the upwind bias of the density coefficient, which is always evaluated at the nth iteration level, allows the simple two- and three-banded matrix form of the AF schemes to be retained over the entire flow field, even in regions of supersonic flow. In fact, use of upwinded density coefficients in any general iteration scheme (i.e., for any arbitrary N operator) could be used to remove the difficulties introduced by type-dependent differencing. The resulting general scheme would retain the same basic differencing (at the $n+1$ iteration level) throughout the entire flow field, relying on the upwind bias of the density (at the nth iteration level) to provide the artificial viscosity in supersonic flow regions. This represents a significant simplification in the handling of supersonic flow regions for transonic flow calculations.

E. α Selection for the Approximate Factorization Schemes

In both the AF1 and AF2 schemes the quantity α is an as yet undefined free parameter. If α were chosen to be Δt^{-1} then both schemes could be

considered to be iterations in pseudo time. This provides one strategy for obtaining fast convergence, namely, advance time as fast as possible with large time steps (i.e., small α's). As pointed out in reference 1, this is effective for attacking the low-frequency errors but not the high-frequency errors. The best overall approach is to use an α sequence containing several values of α. The small values are particularly effective for reducing the low-frequency errors, and the large values are particularly effective for reducing the high-frequency errors. Endpoints for a suitable α sequence can be approximated analytically; for the present case these approximations are given by

AF1: $$\alpha_H = 4\rho/\Delta y^2 \qquad \alpha_L = \rho \tag{30}$$

AF2: $$\alpha_H = 1/\Delta y \qquad \alpha_L = 1 \tag{31}$$

where ρ is a representative value of density (e.g., ρ_∞), and Δy is the minimum y-direction spacing in the finite-difference mesh. Refinement of these estimates by numerical experiment increases the efficiency of the iteration procedure. The α sequence used in the present study is given by

$$\alpha_k = \alpha_H\left(\frac{\alpha_L}{\alpha_H}\right)^{(k-1)/(M-1)} \qquad k = 1, 2, \ldots, M \tag{32}$$

where M is the number of elements in the sequence. This (geometric) sequence has been found to be effective (ref. 1), although other sequences could perhaps provide equivalent or improved convergence performance.

IV. TWO-DIMENSIONAL RESULTS

The three schemes presented in the previous section (SLOR, AF1, and AF2) are evaluated in this section. A two-dimensional, 10% thick circular-arc airfoil with small-disturbance boundary conditions is used as a test case. Both subcritical (Case A) and supercritical (Case B) Mach numbers are considered (see table 1). The finite-difference grid is Cartesian with variable spacing in both the x and y directions, as shown in figure 3. Use of the Cartesian grid with small-disturbance boundary conditions was motivated from the standpoint of simplicity and does not reflect the desired ultimate use of the full potential schemes under investigation.

The subcritical and supercritical pressure coefficient distributions (Cases A and B, respectively) are presented in figure 4. These results were computed with a 90 × 24 mesh containing 47 points on the airfoil surface. The boundaries were located 5 chord-lengths away from the airfoil in the x direction and 6 chord-lengths away in the y direction. In the AF cases, the α sequence contained eight elements (M=8).

A. Convergence Performance for the Subcritical Case

Convergence characteristics for the subcritical case in terms of maximum residual histories are displayed in figure 5. The AF results were established by plotting the maximum residual every eighth iteration, which always corresponded to $\alpha = \alpha_L$ in the eight element sequence. The SLOR results were established by plotting the residual every 20 iterations. All of the convergence parameters (ω_{SLOR}, α_H, and α_L) have been selected by a trial and error optimization process. (Results for two choices of relaxation parameter ($\omega_{SLOR} = 1.95$ and 1.975) are presented for SLOR. The larger value produced faster convergence for a maximum residual drop greater than four orders of magnitude, while the smaller value produced faster convergence for smaller drops in the residual.) The relaxation factor used in both the AF1 and AF2 schemes (ω in eqs. (27) and (29)) was held fixed at 2 for all test cases. Based on a six order of magnitude drop in maximum residual, the AF1 scheme is about twice as fast as the AF2 scheme, and about 16 times faster than the SLOR scheme. These speed ratios are in terms of iteration count. The AF1 and AF2 schemes take about 50% and 30% more CPU time per iteration than SLOR. This should be taken into account when considering the speed ratios based on the total amount of computational work.

For several reasons, exact determination of speed ratios for these schemes is difficult to assess. Firstly, use of grid sequences usually provides as much as a factor of 2 speed increase for SLOR schemes, but only a small speed increase for the AF schemes (ref. 1). Grid sequences were not used for any results reported here. Secondly, use of nonoptimal convergence parameters does slow convergence by as much as a factor of 2 or more for both the SLOR and AF schemes. Because the AF schemes have two parameters to optimize (α_H and α_L), as opposed to only one for SLOR (ω_{SLOR}), optimization is more difficult for the AF schemes. Finally, and most importantly, the AF schemes reduce the errors associated with all frequencies equally well, approximately, while the SLOR scheme is efficient for only the high frequencies. Since the residual is heavily biased toward the high frequency end of the error spectrum, using a specified drop in the maximum residual to define convergence heavily favors the SLOR scheme (ref. 2). More discussion on this last point is provided in this section, part C.

B. Convergence Performance for the Supercritical Case

Convergence characteristics for the supercritical case (Case B) in the form of maximum residual histories are displayed in figure 6. Again the ω_{SLOR}, α_H, and α_L values have been obtained by trial and error optimization. Based on a six order of magnitude drop in the maximum residual and in terms of iteration count, AF2 is slightly more than twice as fast as AF1, and about 11 times faster than SLOR.

The number of supersonic points (NSP) plotted versus iteration number for Case B is shown in figure 7. The final NSP is 187. The AF2, AF1, and SLOR results reach this level in 29, 103, and 320 iterations, respectively. The

small number of iterations required by AF2 to establish the supersonic zone is another indication of how rapidly the solution evolves with this approach.

The AF2 scheme was relatively consistent in convergence speed for both the subsonic and supersonic cases (79 and 118 iterations, respectively). The AF1 scheme, on the other hand, displayed remarkable speed for the subsonic case (39 iterations) but was a disappointment for the supersonic case (254 iterations). Perhaps this is because the ϕ_{xt} error term produced by the AF2 factorization is more suitable for supersonic regions than the ϕ_t error term resulting from the AF1 factorization.

It should be pointed out that use of the standard definition for ν in two dimensions (see eq. (10)) produced pre-shock overshoots which often resulted in numerical instability. This instability was experienced for both the standard rotated (see eq. (17)) and nonrotated difference schemes. (The nonrotated difference scheme simply has no y-direction artificial viscosity term. This causes the term $(\rho\phi_y)_y$ to remain centrally differenced in supersonic regions.) Therefore, an alternative definition for ν was introduced,

$$\nu = \begin{bmatrix} 1 - \left(\frac{\rho}{\rho_*}\right)^{\sigma_e} & M > 0 \\ 0 & M < 1 \end{bmatrix} \tag{33}$$

where ρ_* is the sonic value of density and σ_e has been chosen by numerical experiment to be six. Use of equation (33) instead of the standard definition for ν increases the amount of upwinding or, equivalently, the amount of artificial viscosity in supersonic flow regions. Shock wave overshoots were thereby prevented for the supercritical case presented here.

Several variations of the artificial viscosity term have been investigated. In all cases, only the x-direction artificial viscosity term has been included (i.e., nonrotated differencing). Two of these variations are given by

$$-\overleftarrow{\delta}_x \nu_{i,j} u_{i,j} \rho_{x_{i,j}} \tag{34}$$

and

$$-\overleftarrow{\delta}_x \nu_{i+(1/2),j} u_{i+(1/2),j} \rho_{x_{i,j}} \tag{35}$$

The artificial viscosity term introduced previously (eq. (15)) corresponds exactly to the term reported by Jameson (ref. 3). This form is incorrectly reported in that Jameson actually uses the artificial viscosity given by equation (34) (private communication from A. Jameson, Courant Institute of Mathematical Sciences, N.Y.). The artificial viscosity term given by equation (35) is still another successful version. All three variations of artificial viscosity (with suitably tailored forms for ν) have been tested for Case B and give essentially the same results.

C. Residual vs Error

Relative levels of convergence for AF2 and SLOR for given reductions in maximum residual are compared in figure 8. The solid line represents the final solution, which has been converged until the maximum residual dropped six orders of magnitude. The other results represent intermediate AF2 and SLOR solutions in which the maximum residual has been reduced by one, two, and three orders of magnitude. It is immediately obvious that reducing the maximum residual by equal amounts for AF2 and SLOR does not produce intermediate results with the same level of error. In fact, the error reduction for these two schemes can be substantially different for the same degree of residual reduction. For instance, the AF2 solution after a two order of magnitude reduction in maximum residual (fig. 8(b)) is closer to the final solution than the SLOR solution is after a residual drop of three orders of magnitude (fig. 8(c)).

This behavior can also be observed by comparing the maximum residual history curves of figure 6 with the RMS error history curves given in figure 9. The RMS error at iteration n (E^n_{RMS}) was computed from the surface pressure coefficient distribution by the following formula

$$E^n_{RMS} = \left[\frac{\sum_{i=i_{LE}}^{i_{TE}} \left(C^n_{p_i} - \bar{C}_{p_i} \right)^2}{i_{TE} - i_{LE} + 1} \right]^{1/2} \tag{36}$$

were $C^n_{p_i}$ is the surface pressure coefficient at the ith grid point and the nth iteration, $\bar{C}_{p_i}$ is the surface pressure coefficient at the ith grid point taken from the converged solution, and i_{LE} and i_{TE} are the indices indicating the leading and trailing edge grid points. The SLOR residual drops very rapidly initially and then levels off. The SLOR RMS error drops gradually. Therefore, at the "knee" in the residual history curve, even though the residual has dropped by about three orders of magnitude, the actual RMS error has dropped by only one order of magnitude. In contrast, both maximum residual and RMS error results for the AF schemes are nearly straight lines with about the same slope.

This behavior is the result of two factors (ref. 2): (1) the AF2 scheme treats all error components equally well (approximately), whereas the SLOR scheme performs efficiently on only the high-frequency error components; and (2) it can be shown that the residual is a weighted sum of errors, over the entire error frequency spectrum, weighted by the eigenvalue of the finite difference scheme. The eigenvalue for the high-frequency error components is $O(\Delta x^{-2})$, while the eigenvalue for the low-frequency error components is $O(1)$. Hence, the residual is heavily influenced by the high-frequency errors. During the initial phase of a calculation, equal residual drops for AF2 and SLOR indicate the same drop in high frequency error, but the reduction rates for the low-frequency errors are significantly different. For this reason the AF

approach reduces the total error much faster, and consequently, the solution evolves much more rapidly. Therefore, the maximum residual operator should not be used as the basis for comparison between AF and SLOR schemes. RMS errors are much better suited for this purpose. In practice, use of the maximum residual operator for either AF or SLOR is the most convenient method for monitoring convergence (since the error is unknown). However, the convergence criterion must be adjusted in accordance with the solution procedure in use.

D. Use of Nonoptimal Convergence Parameters

Only "optimal" convergence (i.e., cases with convergence parameters adjusted for optimal convergence) have been considered thus far. Because in practice the optimal values for α_H, α_L, and ω_{SLOR} are not known a priori, it is of interest to know the effect of nonoptimal parameters on the convergence speed. The RMS error histories for AF1, AF2, and SLOR for nonoptimal parameters are shown in figure 10. The nonoptimal SLOR relaxation factor was chosen to be 1.8, and the α_H and α_L parameters for AF1 and AF2 were chosen from equations (30) and (31). For a four order of magnitude reduction in RMS error (which is well beyond plottable accuracy) nonoptimal AF2 is approximately 2.5 times slower than the optimal AF2 results. The AF1 and SLOR results are similarly affected, being about 1.5 and 3 times slower, respectively. For the nonoptimal case, in terms of iteration count, AF2 is about 1.5 times faster than AF1 and about 12 times faster than SLOR. In terms of actual computer time, AF2 is about 1.7 times faster than AF1 and nearly an order of magnitude faster than SLOR.

Another indication of how fast the AF2 scheme can establish the global solution even for nonoptimal acceleration parameters is shown in figure 11. The solid line in each case is the final solution, which has been converged until the maximum residual dropped six orders of magnitude. The other results presented are AF2 and SLOR intermediate solutions in which the maximum residual has been reduced by one, two, and three orders of magnitude. As before (fig. 8), it is again obvious that reducing the maximum residual by equal amounts for AF2 and SLOR solutions does not produce equivalent error reduction. In the present nonoptimal case, the difference between the AF2 and SLOR solutions for a given drop in residual is even larger than in the previous optimum case. This is because the smaller value of ω_{SLOR} used in the nonoptimum case puts even more emphasis on the high-frequency errors, thus causing the SLOR residual to drop faster, while the RMS error is dropping slower.

Obtaining nearly optimal α-sequence endpoints (α_L, α_H) for the AF2 scheme is not difficult. The most important influence on the α values is the finite-difference mesh. If the mesh remains fixed from one case to another, then the same α's will still be approximately optimum. If the mesh does change, estimates for the new optimal α endpoints $(\alpha_L^{new}, \alpha_H^{new})$ can be obtained (from eq. (31)) as follows:

$$\alpha_L^{new} = \alpha_L^{old}$$

$$\alpha_H^{new} = \alpha_H^{old} \, \Delta y_{min}^{old} / \Delta y_{min}^{new} \tag{37}$$

where α_L^{old} and α_H^{old} are the old hand-optimized (trial and error) endpoints, and Δy_{min}^{old} and Δy_{min}^{new} are the minimum Δy spacings in the old and new meshes, respectively. This philosophy has been tried in a limited number of cases, and seems to be acceptable. However, because of the limitations of the present formulation (nonlifting and small disturbance boundary conditions) more investigation is needed.

V. CONCLUSIONS

New fully implicit algorithms for solving the full potential equation in conservation form have been developed. These new schemes are of the approximate-factorization variety. Computed results indicate a substantial increase in computational efficiency over an SLOR algorithm.

The spatial difference scheme used to approximate the full potential equation is equivalent to the one developed by Jameson. However, in the present approach, the artificial viscosity required to maintain stability in supersonic regions is not added explicitly. It is introduced by spatially retarding the density in the finite-difference equation. This strategy greatly simplifies the solution procedure, so that only bidiagonal or tridiagonal matrix operations are required.

Results indicate that the standard measure of convergence (i.e., a specified reduction in the maximum residual) is not a good means for comparing AF and SLOR convergence rates. Using the maximum residual as a criterion to determine relative levels of convergence for either technique individually, is not questioned. However, AF schemes definitely reach a greater degree of convergence in terms of the error at higher residuals than do SLOR techniques.

The new AF schemes although applied in this report only to circular-arc airfoils with small-disturbance boundary conditions and Cartesian finite-difference grids, are extendible to arbitrary geometries in both two- and three-dimensional flows. The principal difficulty is the handling of the cross derivative terms arising from general geometry transformations. Solutions for cases with airfoil adapted grids have been obtained, and the efficiency of the AF procedure does carry over to these more practical flows. Details are presented in a report in preparation by T. L. Holst.

REFERENCES

1. Ballhaus, W. F.; Jameson, A.; and Albert, J.: Implicit Approximate Factorization Schemes for the Efficient Solution of Steady Transonic Flow Problems. AIAA Paper 77-634, June 1977.

2. Ballhaus, W. F.: A Fast Implicit Solution Procedure for Transonic Flows. Presented at the Third International Symposium on Computing Methods in Applied Sciences and Engineering, Versailles, France, Dec. 5-9, 1977.

3. Jameson, A.: Transonic Potential Flow Calculations Using Conservative Form. AIAA Second Computational Fluid Dynamics Conf. Proc., June 1975, pp. 148-155.

4. Steger, J. L.; and Baldwin, B. S.: Shock Waves and Drag in the Numerical Calculation of Isentropic Transonic Flow. NASA TN D-6997, 1972.

5. Lax, P. D.: Weak Solutions of Nonlinear Hyperbolic Equations and Their Numerical Computation. Communications on Pure and Applied Mathematics, vol. 7, 1954, pp. 159-193.

6. Murman, E. M.: Analysis of Embedded Shock Waves Calculated by Relaxation Methods. Proceedings of AIAA Computational Fluid Dynamics Conference, Palm Springs, July 1973.

7. Jameson, A.: Transonic Flow Calculations, VKI Lecture Series: Computational Fluid Dynamics, von Karman Institute for Fluid Dyanamics, Rhode-St-Genese, Belgium, March 15-19, 1976.

8. Ballhaus, W. F.; and Steger, J. L.: Implicit Approximate Factorization Schemes for the Low-Frequency Transonic Equation. NASA TM X-73,082, 1975.

TABLE 1.- TABULATION OF SOLUTION PARAMETERS

	Case[a]	Scheme	ω_{SLOR}	α_L	α_H
Optimum	A	SLOR	1.975	---	---
		AF1	---	0.04	100,000
		AF2	---	.4	100
Optimum	B	SLOR	1.95	---	---
		AF1	---	1.3	4,000
		AF2	---	.6	60
Nonoptimum	B	SLOR	1.8	---	---
		AF1	---	.8	128,000
		AF2	---	1.0	200

[a]Case A: $M_\infty = 0.7$ (subcritical); Case B: $M_\infty = 0.84$ (supercritical).

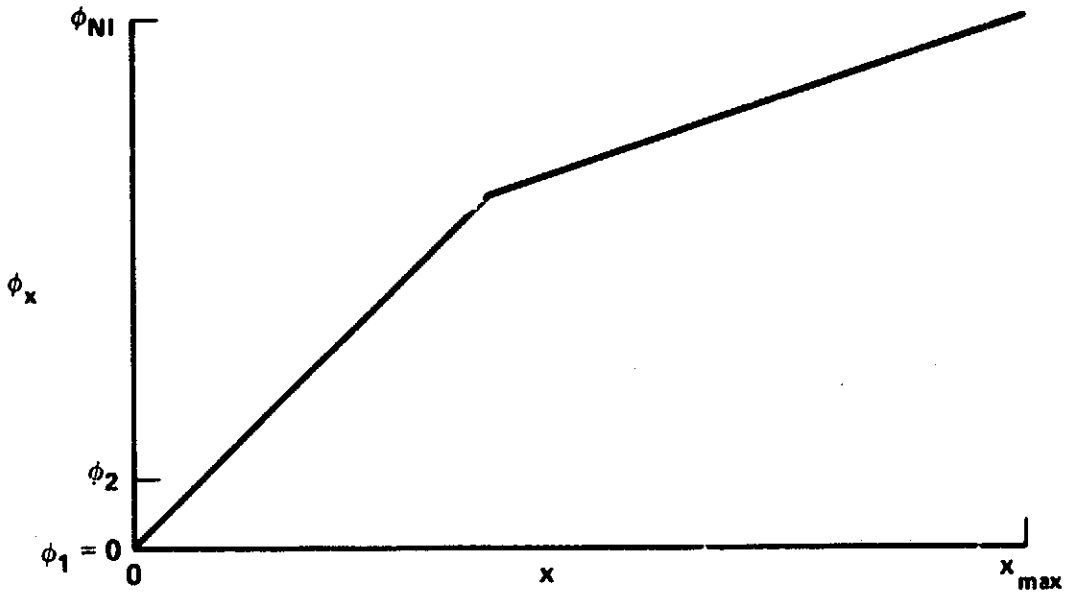

a) ϕ PROFILE

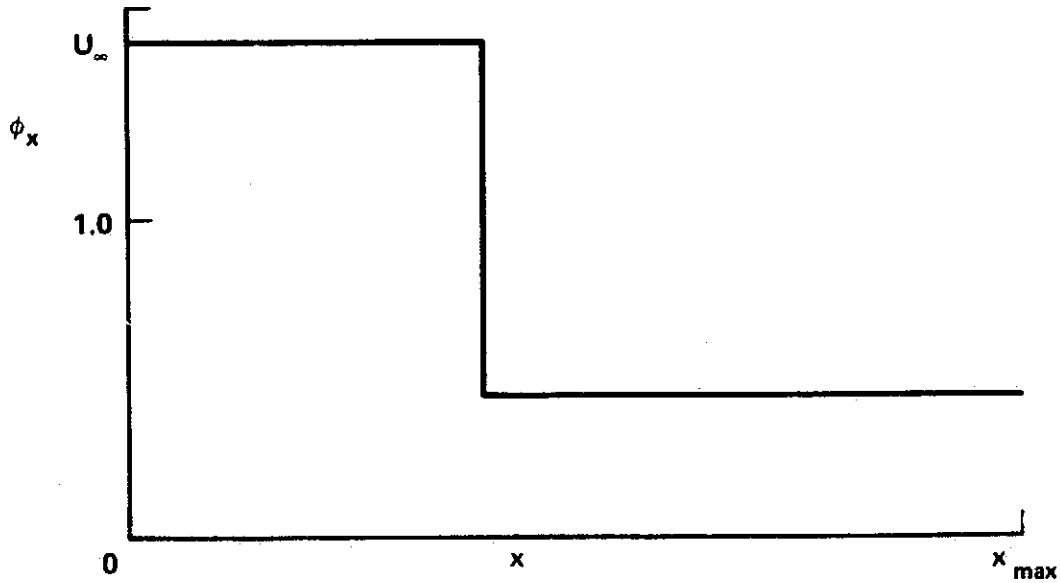

b) ϕ_x PROFILE

Figure 1.- One-dimensional full potential equation solution.

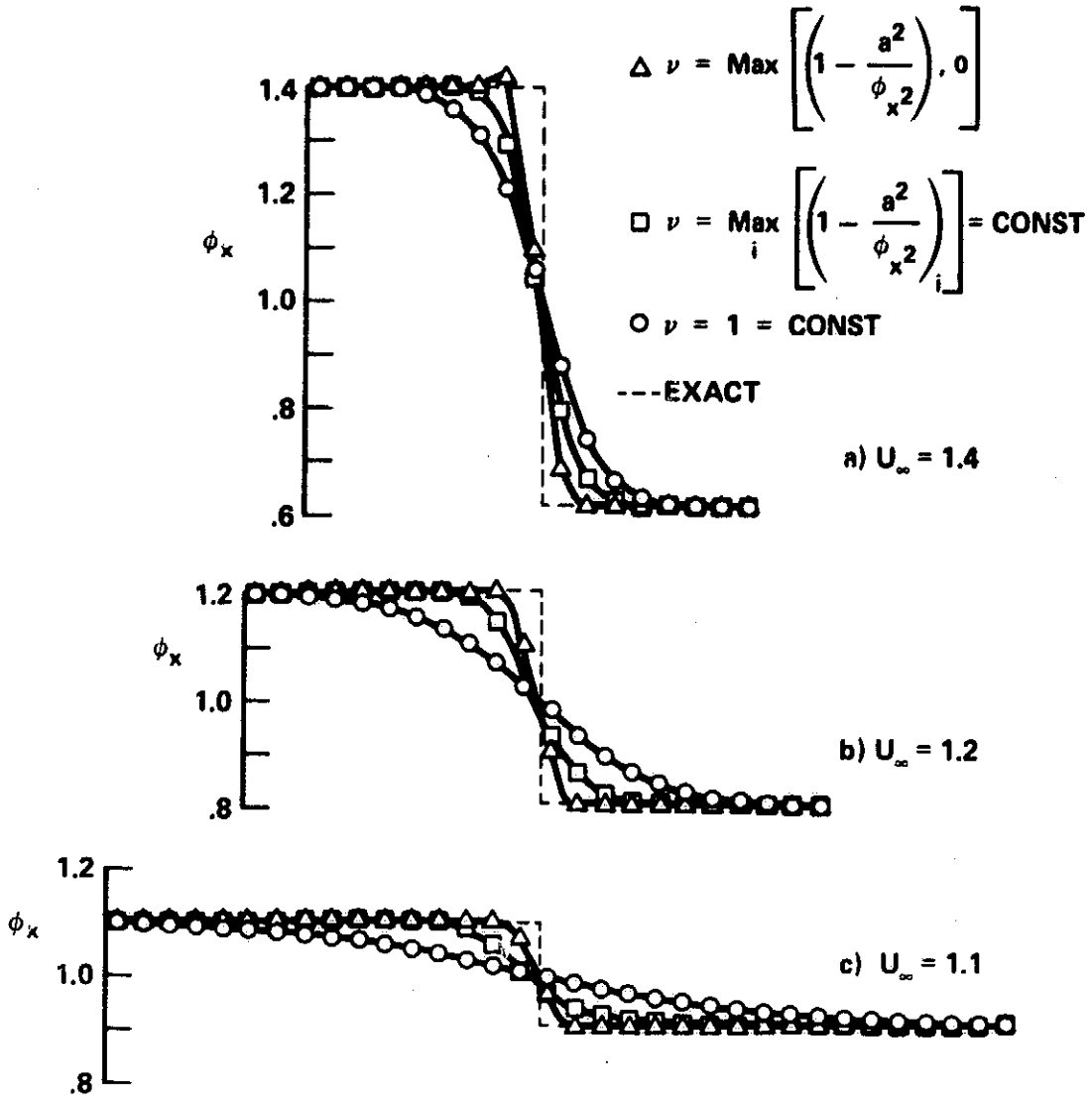

Figure 2.- Shock profiles, ϕ_x vs x.

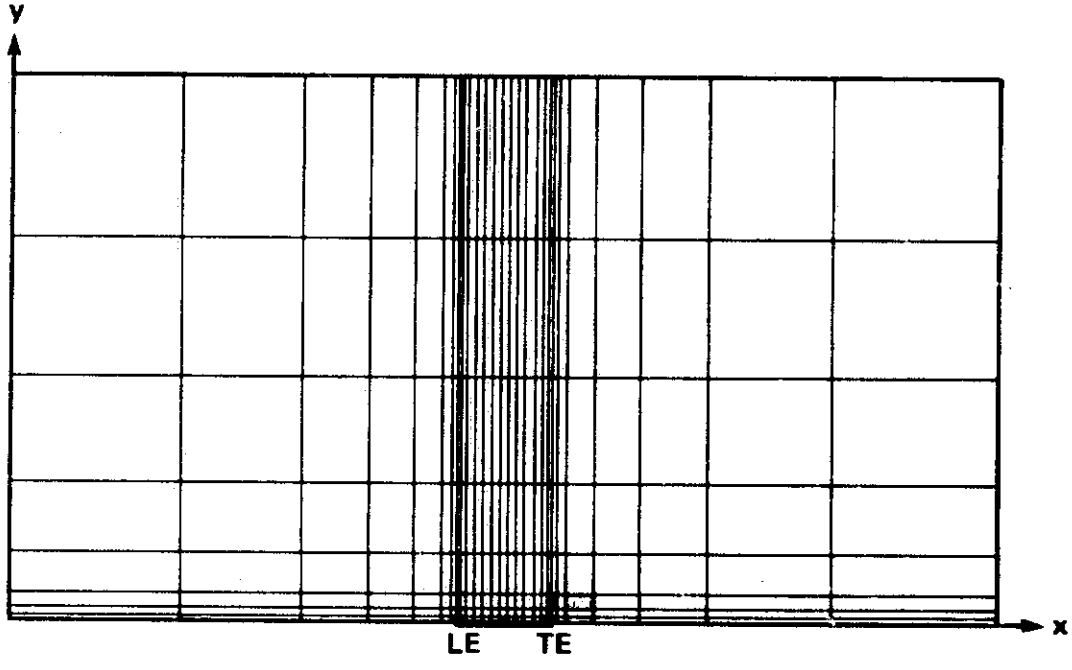

Figure 3.- Finite-difference mesh (two dimensions).

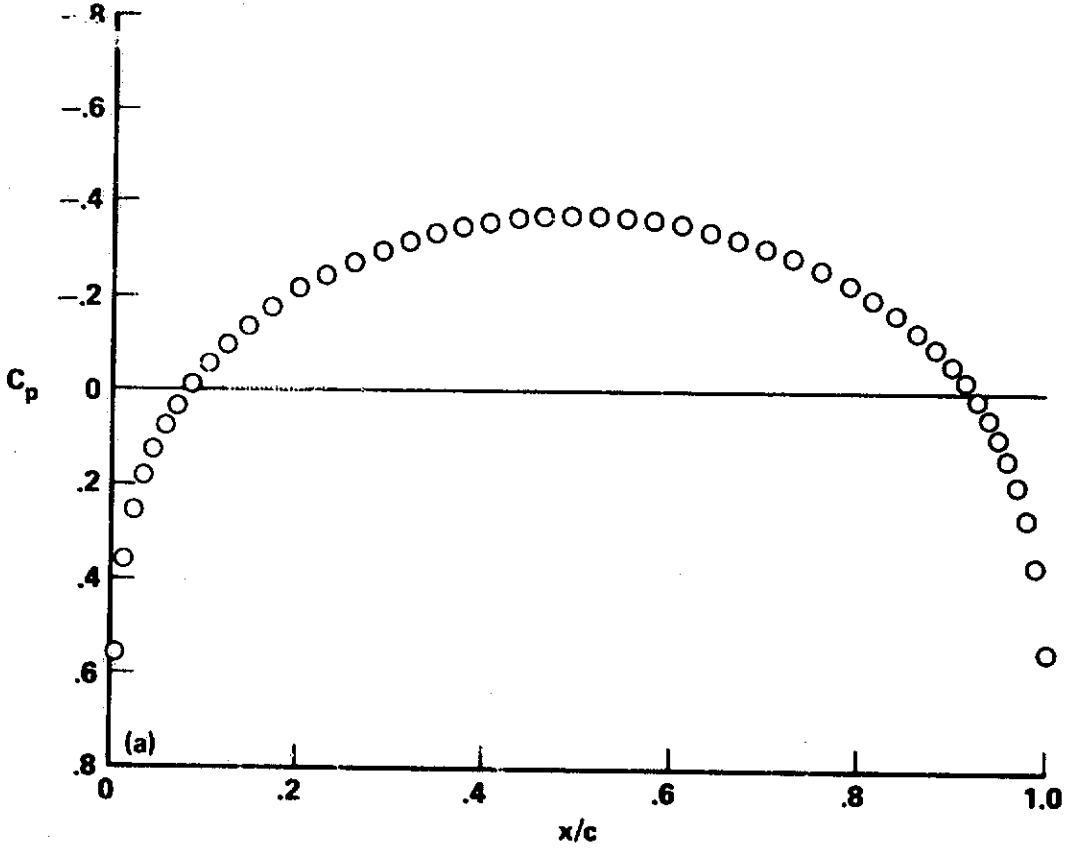

(a) Subcritical case (Case A, $M_\infty = 0.7$).

Figure 4.- 10% circular arc pressure coefficient distributions.

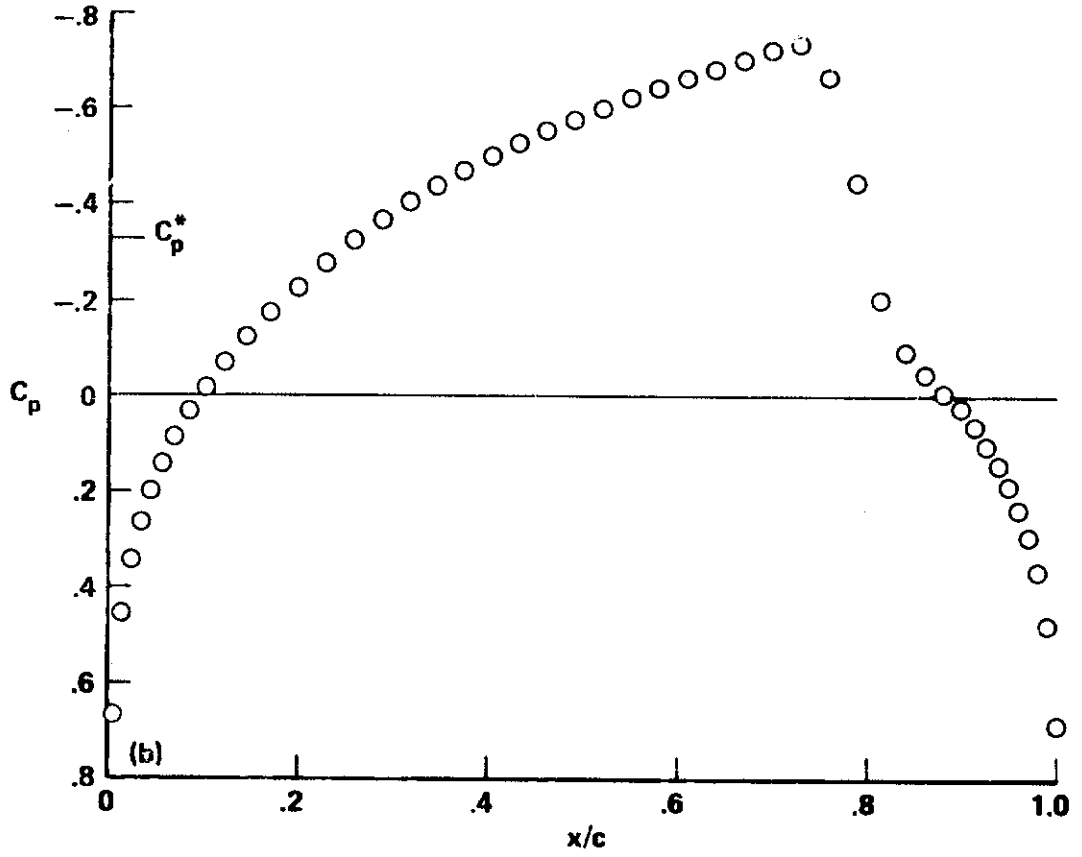

(b) Supercritical case (Case B, $M_\infty = 0.84$).

Figure 4.- Concluded.

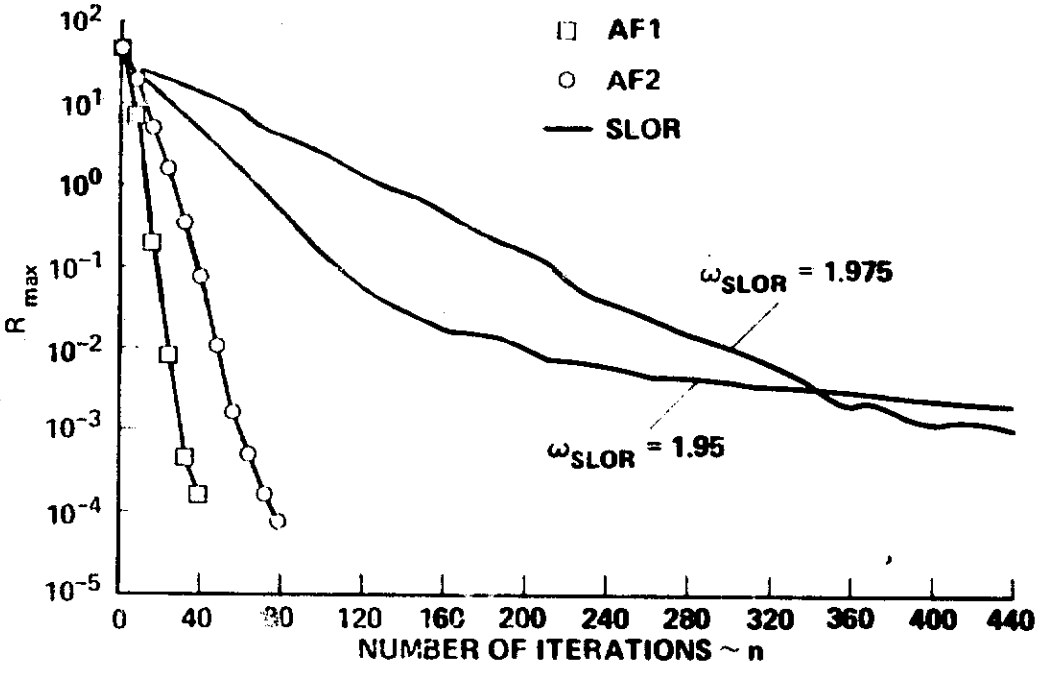

Figure 5.- Maximum residual convergence history comparison (Case A).

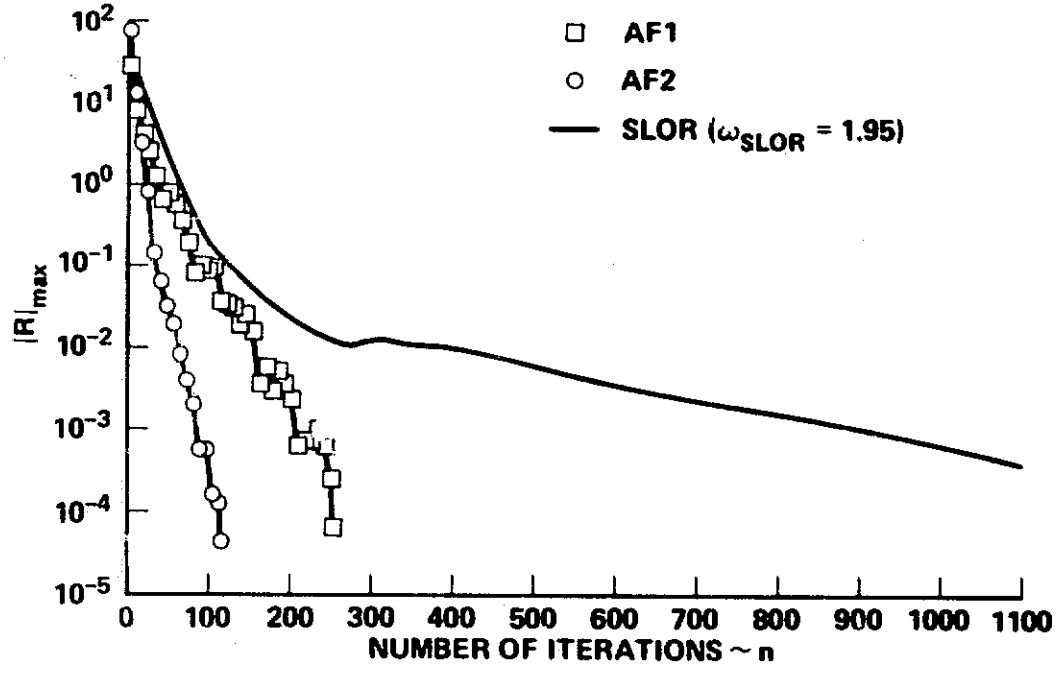

Figure 6.- Maximum residual convergence history comparison (Case B).

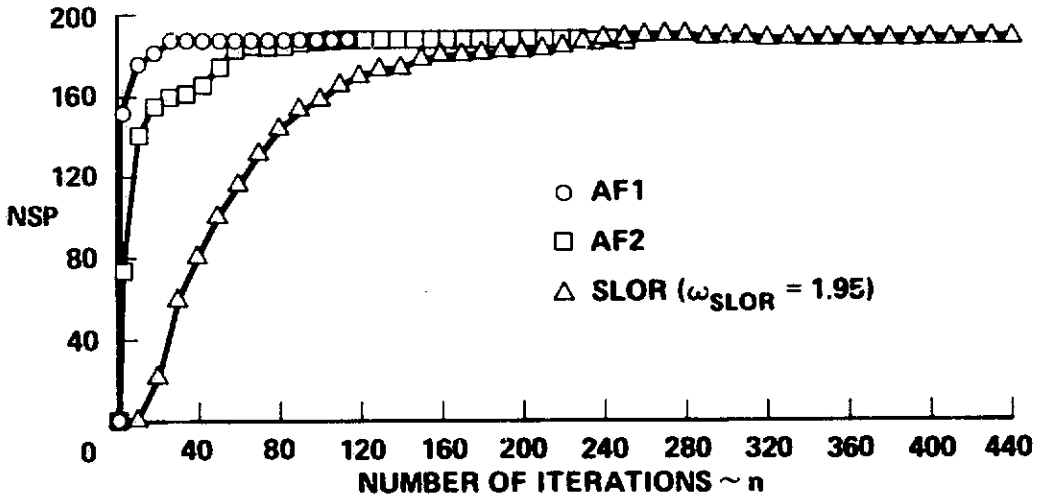

Figure 7.- Development of the supersonic region (Case B).

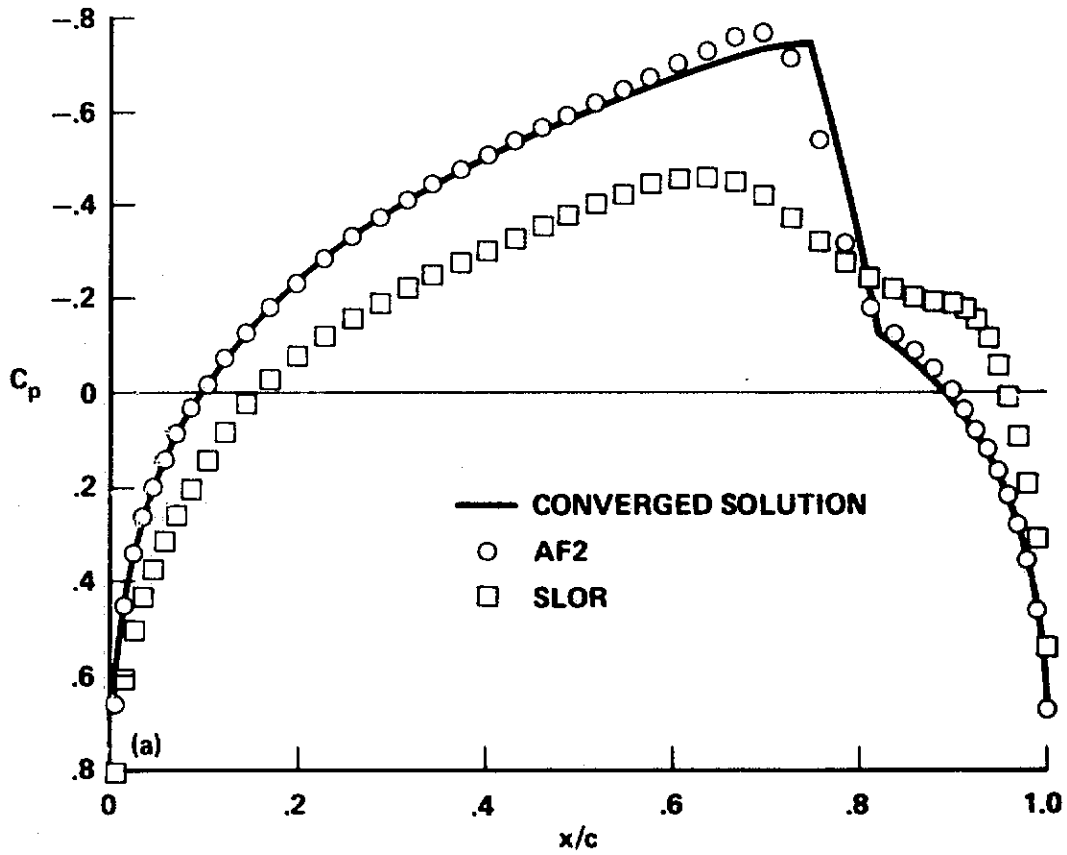

(a) $|R|_{max}$ reduced one order of magnitude.

Figure 8.- Intermediate solution comparisons after specified reductions in the maximum residual (Case B, optimum convergence).

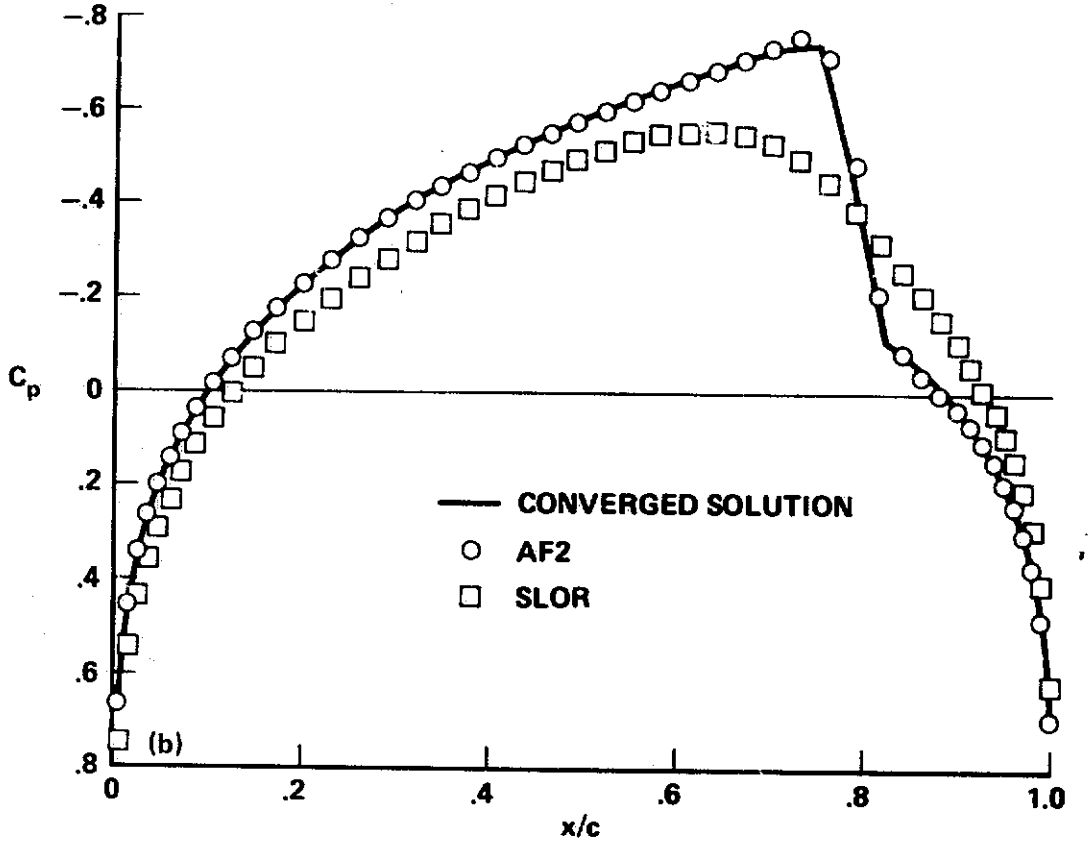

(b) $|R|_{max}$ reduced two orders of magnitude.

Figure 8.- Continued.

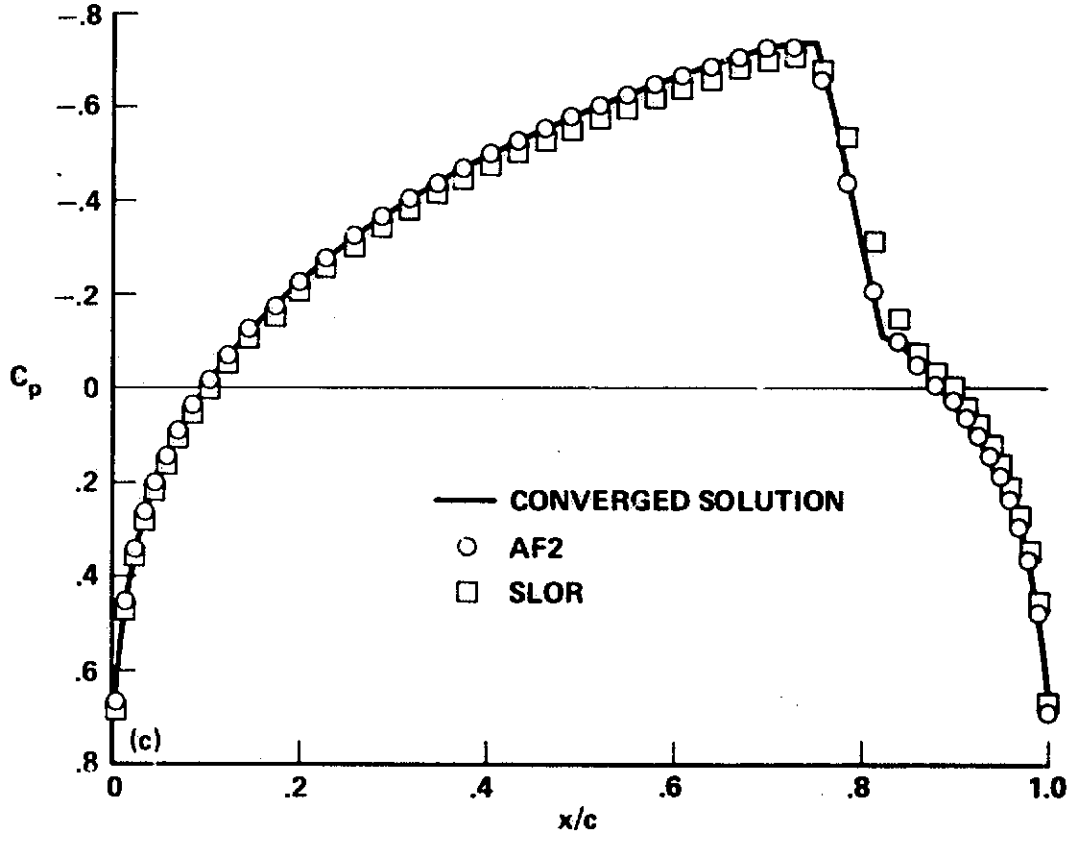

(c) $|R|_{max}$ reduced three orders of magnitude.

Figure 8.- Concluded.

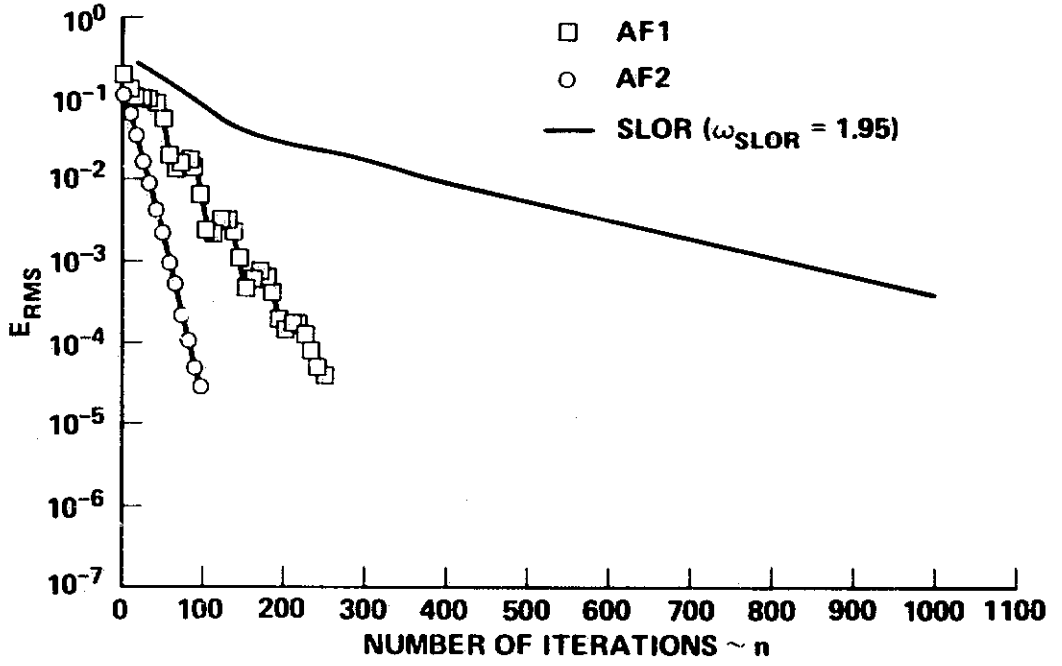

Figure 9.- RMS error convergence history comparison (Case B).

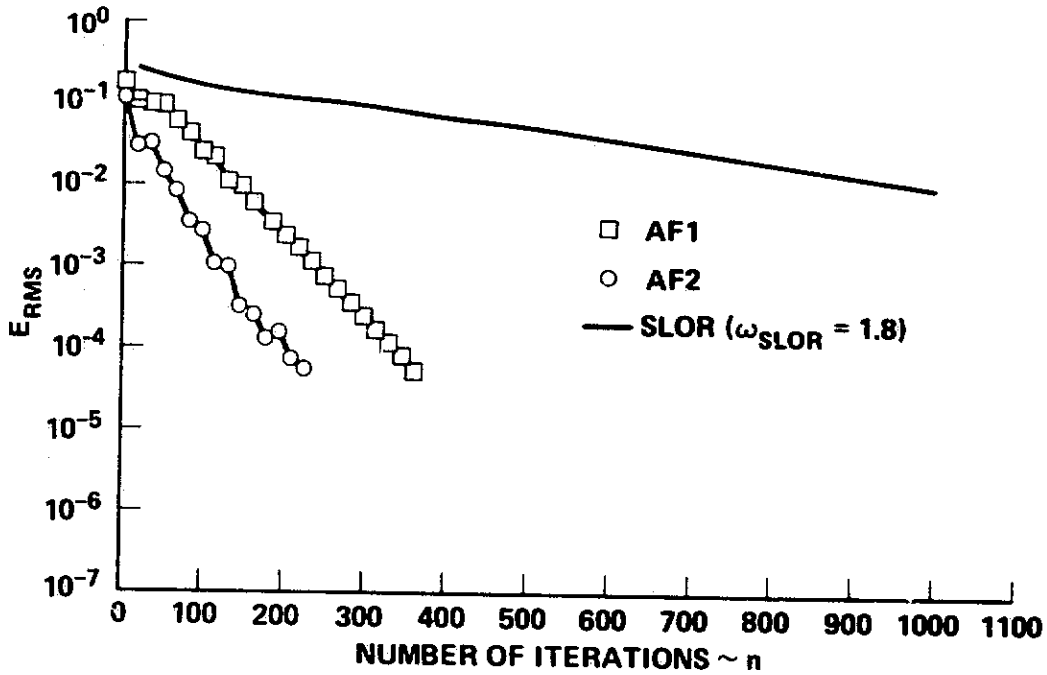

Figure 10.- RMS error convergence history comparison (Case B, nonoptimal convergence).

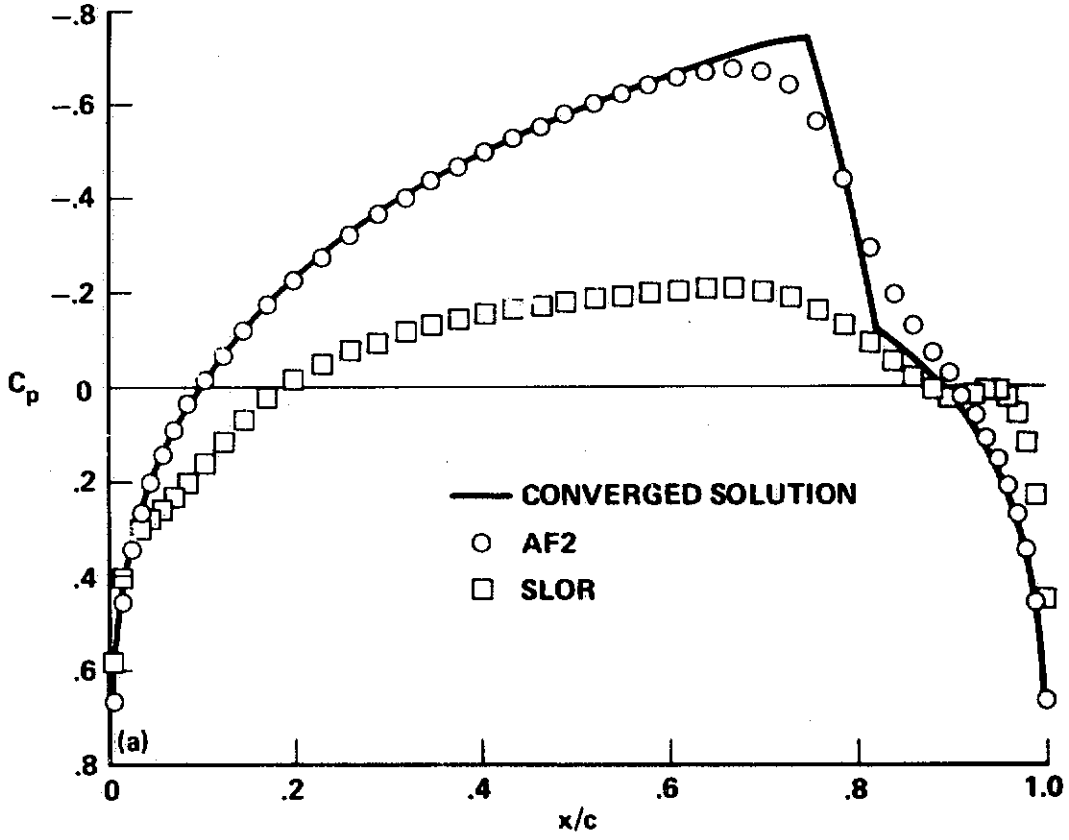

(a) $|R|_{max}$ reduced one order of magnitude.

Figure 11.- Intermediate solution comparisons after specified reductions in the maximum residual (Case B, nonoptimal convergence).

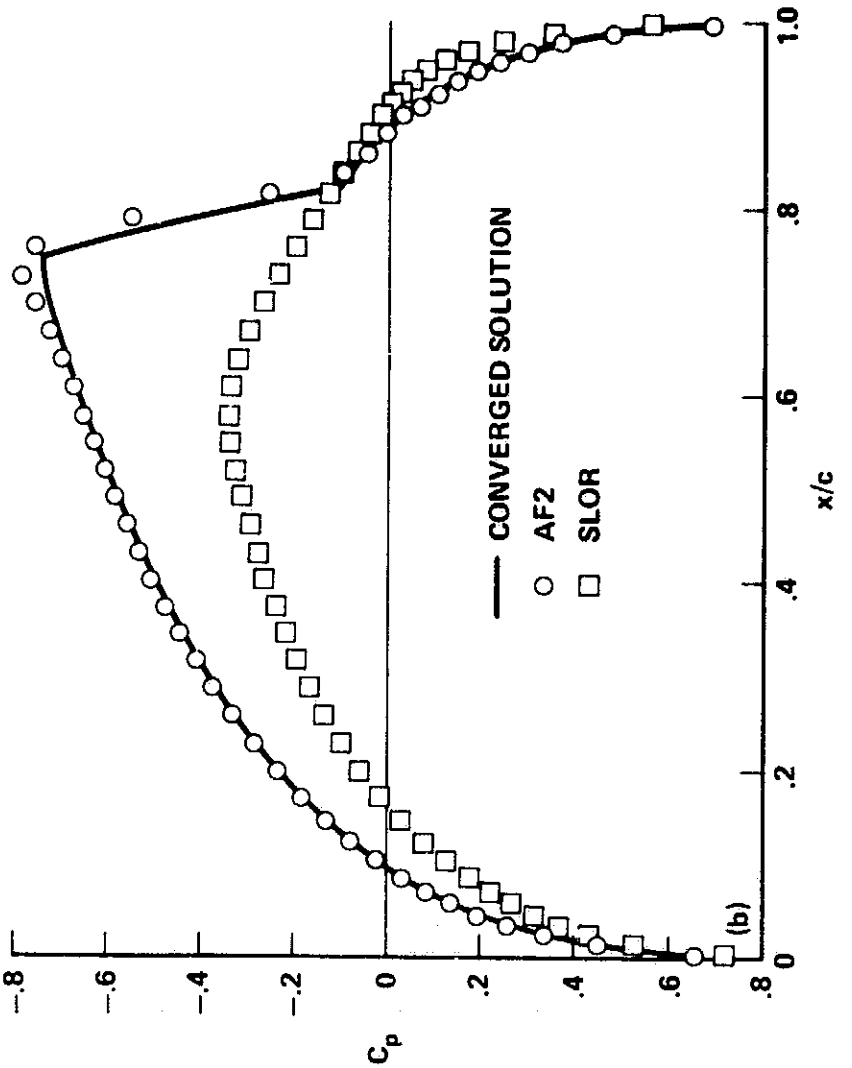

(b) $|R|_{max}$ reduced two orders of magnitude.

Figure 11.- Continued.

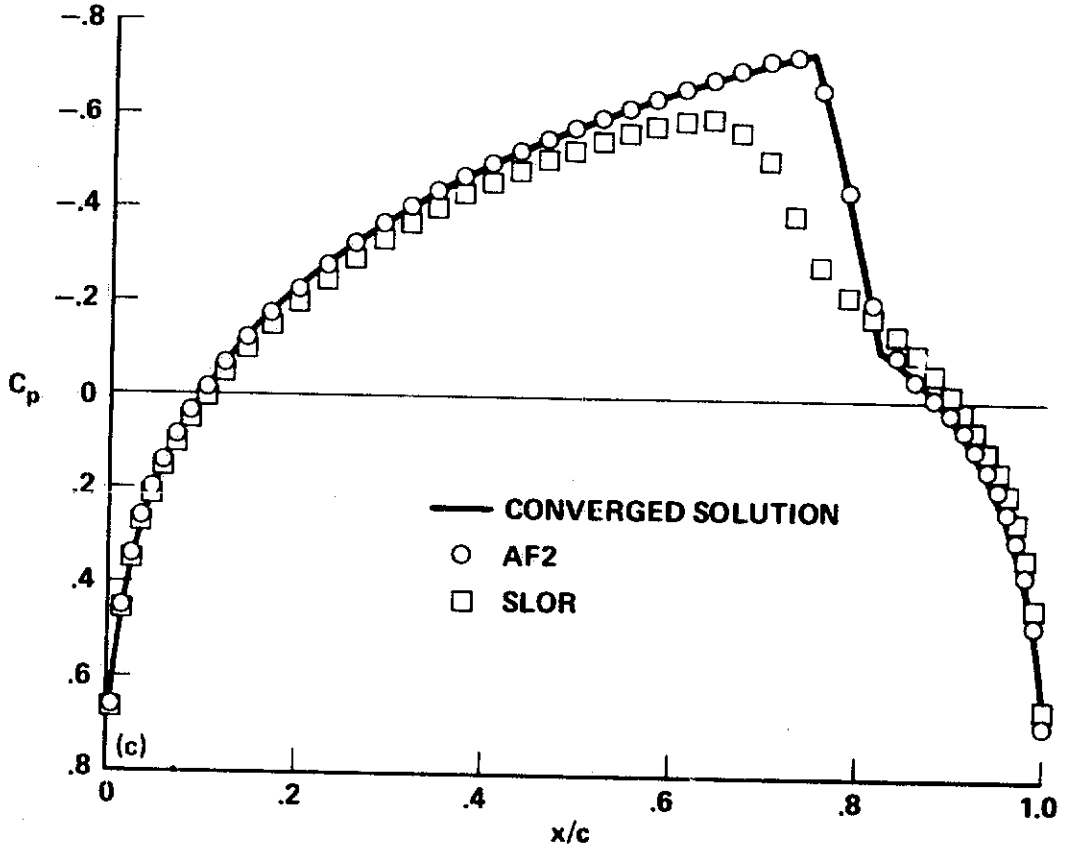

(c) $|R|_{max}$ reduced three orders of magnitude.

Figure 11.- Concluded.

1. Report No.	2. Government Accession No.	3. Recipient's Catalog No.
NASA TM-78469		

4. Title and Subtitle	5. Report Date
CONSERVATIVE IMPLICIT SCHEMES FOR THE FULL POTENTIAL EQUATION APPLIED TO TRANSONIC FLOWS	6. Performing Organization Code

7. Author(s)	8. Performing Organization Report No.
Terry L. Holst and William F. Ballhaus	A-7338
	10. Work Unit No. 505-06-11

9. Performing Organization Name and Address	11. Contract or Grant No.
NASA Ames Research Center and Aeromechanics Laboratory, U.S. Army Aviation R&D Command, Ames Research Center, Moffett Field, Calif. 94035	

12. Sponsoring Agency Name and Address	13. Type of Report and Period Covered
National Aeronautics and Space Administration, Washington, D.C. 20546, and U.S. Army Aviation R&D Command, Ames Research Center, Moffett Field, Calif. 94035	Technical Memorandum
	14. Sponsoring Agency Code

15. Supplementary Notes

16. Abstract

Implicit approximate factorization techniques (AF) are investigated for the solution of matrix equations resulting from finite-difference approximations to the full potential equation in conservation form. For transonic flows, an artificial viscosity, required to maintain stability in supersonic regions, is introduced by an upwind bias of the density. Two implicit AF procedures are presented and their convergence performance is compared with that of the standard transonic solution procedure, successive line overrelaxation (SLOR). Subcritical and supercritical test cases are considered. The results indicate that the AF schemes are substantially faster than SLOR.

17. Key Words (Suggested by Author(s))	18. Distribution Statement
Transonic flow Computational methods	Unlimited STAR Category - 64

19. Security Classif. (of this report)	20. Security Classif. (of this page)	21. No. of Pages	22. Price*
Unclassified	Unclassified	36	$4.00

*For sale by the National Technical Information Service, Springfield, Virginia 22161